Electronic Supplementary Information

Functional nanonetwork-structured polymers with inbuilt poly(acrylic acid) linings for enhanced adsorption

Weicong Mai, Yuan Zuo, Chuanfa Li, Jinlun Wu, Kunyi Leng, Xingcai Zhang, Ruliang Liu, Ruowen Fu and Dingcai Wu*

Materials Science Institute, PCFM Lab and GDHPRC Lab, School of Chemistry, Sun Yat-sen University, Guangzhou 510275, P. R. China

E-mail: wudc@mail.sysu.edu.cn

Experimental Section

Materials. *tert*-Butyl acrylate (*t*BA; Aladdin, 99%) and styrene (St; Aladdin, AR) were purified by passing through a basic alumina column. CuBr (Aladdin, AR) was purified by washing sequentially with acetic acid and ethanol, filtration and drying, and was stored under nitrogen before use. $CuBr_2$ (Aladdin, AR), N,N,N′,N′,N″-pentamethyldiethylenetriamine (PMDETA; Aladdin, 99%), anhydrous aluminum chloride ($AlCl_3$; Aladdin, AR), dichloromethane (Aladdin, HPLC), 3-aminopropyltriethoxysilane (APTES; Aladdin, AR), 2-bromoisobutyryl bromide (BiBB; Aladdin, AR), malachite green (Aladdin, AR), methyl violet (Aladdin, AR), silver nitrate ($AgNO_3$; Aladdin, AR), copper sulfate pentahydrate (Aladdin, AR), lead nitrate (Aladdin, AR), chromium(III) nitrate nonahydrate (Aladdin, AR) and other reagents were used as received.

Synthesis of SiO_2-Br nanospheres. SiO_2 nanospheres were synthesized according to Stöber method. In our synthesis, ethanol (400 mL) and $NH_3 \cdot H_2O$ (25 wt % in water, 21 mL) were mixed in a 500 mL three-necked round-bottom flask, and stirred for 10 min at 40 ℃. Then 20 mL of tetraethyl orthosilicate (TEOS) was added and stirred for 10 h at 40 ℃ to obtain SiO_2 nanospheres with diameter of 54 nm. 4 ml of APTES was dropped in a three-necked flask for 2 h, and then the reaction temperature was raised to 85℃ for 3 h. The solution was centrifuged at 12000 rpm for 10 min, washed with ethanol and dichloromethane twice, respectively, and then dispersed in 180 mL of dichloromethane. After purging with N_2 for 30 min, 8.4 mL of triethylamine was injected into the solution, and then 7.2 mL of BiBB was added at a rate of 14.4 mL h^{-1} at 0℃ under stirring. The solution was stirred at 0℃ for 3 h and then at 30℃ for 48 h. The resulting SiO_2-Br (diameter: 54 nm) was centrifuged at 12000 rpm, washed by THF and acetone/water mixture (1:1) for 3 times, respectively, and finally dried in a vacuum oven at 40℃ overnight. The synthesis procedures of the SiO_2-Br nanospheres with diameters of 89 and 324 nm were exactly the same as those of the above SiO_2-Br with diameter of 54 nm, except 10 and 20 mL water were used at the first step, respectively.

Synthesis of SiO_2-*g*-P*t*BA nanospheres. SiO_2-*g*-P*t*BA_{81} was synthesized according to the following recipe: *t*BA/SiO_2-Br/CuBr/$CuBr_2$/PMDETA =1000/1/4/0.4/4.4 (molar

ratio). SiO_2-Br, $CuBr_2$, PMDETA and *t*BA were stirred in a Schlenk flask under a nitrogen atmosphere for 30 min. Then CuBr was added to the mixture and the solution was stirred under a nitrogen atmosphere for 30 min. The reaction was carried out at 60 °C for 6 h. The polymerization was stopped by opening the flask and exposing the catalyst to air. The resulting SiO_2-*g*-P*t*BA_{81} was precipitated in excess methanol, centrifuged at 12000 rpm for 10 min, and then dried in vacuum at 40 °C overnight (yield: 103%). It should be noted that precipitation, dissolution, washing and centrifugation for several times were needed, thus causing inevitable mass loss. The severe mass loss for SiO_2-*g*-P*t*BA_{81} nanospheres could be mainly ascribed to their incomplete precipitation in methanol.

Synthesis of SiO_2-*g*-P*t*BA-*b*-PS nanospheres. SiO_2-*g*-P*t*BA-*b*-PS nanospheres were synthesized according to the following recipe: St/SiO_2-*g*-P*t*BA-Br/CuBr/$CuBr_2$/PMDETA =1000/1/4/0.4/4.4 (molar ratio). SiO_2-*g*-P*t*BA-Br, $CuBr_2$, PMDETA and St were stirred in a Schlenk flask under a nitrogen atmosphere for 30 min. Subsequently, CuBr was added to the mixture, and the solution was stirred under a nitrogen atmosphere for 30 min. The reaction was carried out at 90 °C. The polymerization was stopped by opening the flask and exposing the catalyst to air after 6, 12 or 24 h to obtain DP_{PS} of 6, 145 or 1218. The product (SiO_2-*g*-P*t*BA_{81}-*b*-PS_6, SiO_2-*g*-P*t*BA_{81}-*b*-PS_{145} or SiO_2-*g*-P*t*BA_{81}-*b*-PS_{1218}) was precipitated in excess methanol, washed by THF for three times, centrifuged, and dried in vacuum at 40 °C overnight (yield: 48%, 160% or 735%, respectively). It should be noted that precipitation, dissolution, washing and centrifugation for several times were needed, thus causing inevitable mass loss. The severe mass loss for SiO_2-*g*-P*t*BA_{81}-*b*-PS_6 nanospheres could be mainly ascribed to their incomplete precipitation in methanol.

Preparation of FNNSP-PAA products. $AlCl_3$ (0.84 g) and CCl_4 (18 mL) was stirred in a 50 mL three-necked round-bottom flask for 30 min. The temperature was raised to 75°C, and then SiO_2-*g*-P*t*BA_{81}-*b*-PS_{1218} (0.3 g) was added under stirring to conduct the hypercrosslinking for 24 h. The product was filtered, washed three times with a mixture of acetone and hydrochloric acid, and then dried in vacuum at 40 °C. The resulting SiO_2-*g*-PAA_{81}-*b*-*x*PS_{1218} was etched with HF, thus obtaining the target FNNSP-PAA

product FNNSP-PAA_{81}-*b*-PS_{1218}. Other FNNSP-PAA products were also prepared according to the above method.

Characterization. The nanostructures of the samples were investigated by a Hitachi S-3400 scanning electron microscope (SEM) and a FEI Tecnai G2 Spirit transmission electron microscope (TEM). FTIR spectra were conducted at room temperature on a Bruker Equinox 55 Fourier transform infrared spectroscopy. The molecular weight and molecular weight distribution of the polymers were measured on a Waters gel permeation chromatography (GPC). Molecular weights were calibrated based on polystyrene standards. THF was used as an eluent at a flow rate of 1.0 mL min^{-1}. The ^1H NMR spectrum was conducted by a 400 MHz Bruker advance III spectrometer. N_2 adsorption measurements were carried out using a Micromeritics ASAP 2020 analyzer at 77 K. The BET surface area (S_{BET}) was determined by Brunauer-Emmett-Teller (BET) theory. The micropore surface area (S_{mic}) and meso-/macropore surface area (S_{ext}) were determined by t-plot method. The pore size distribution was analyzed by original density functional theory (DFT) combined with non-negative regularization and medium smoothing. The total pore volume (V_{total}) was calculated according to the amount adsorbed at a relative pressure P/P_0 of about 0.99. Thermogravimetric analysis (TGA) was conducted on a NETZSCH TG 209F1 Iris instrument. The grafting density of hairy nanospheres was calculated according to a reported method.[1]

Adsorption experiments toward malachite green and methyl violet. The concentration of malachite green and methyl violet was detected by Shimadzu UV-Vis-NIR spectrophotometer. Malachite green and methyl violet adsorption experiments were performed as follows. FNNSP-PAA_{81}-*b*-PS_{1218} (25 mg) was soaked into a solution (water/ethanol=24/1) of malachite green or methyl violet (40 ml, 100 mg L^{-1}), and vibrated in a thermostatic shaker at 25 °C. At predetermined time intervals, 0.3 ml of solution was taken and diluted for UV-Vis test. The adsorption capacity was calculated by measuring malachite green or methyl violet concentration before and after adsorbed by FNNSP-PAA_{81}-*b*-PS_{1218}. NNSP-PS was subjected to the same adsorption procedure described above and used as a control.

Adsorption experiments toward heavy metal ions. The concentration of heavy metal

ions was detected by a PerkinElmer Optima 8300 inductively coupled plasma optical emission spectrometry (ICP-OES). Adsorption experiments toward heavy metal ions were performed as follows: FNNSP-PAA_{81}-*b*-PS_{1218} (4 mg) was added into an aqueous solution of Cu^{2+}, Ag^{+}, Pb^{2+} or Cr^{3+} (10 ml, 10 ppm), and stirred at 25 °C for 24 h. Then the solution was withdrawn and filtrated for ICP-AES test. The adsorption capacity was calculated by measuring concentrations of heavy metal ions before and after adsorbed by FNNSP-PAA_{81}-*b*-PS_{1218}. NNSP-PS was subjected to the same adsorption procedure described above and used as a control.

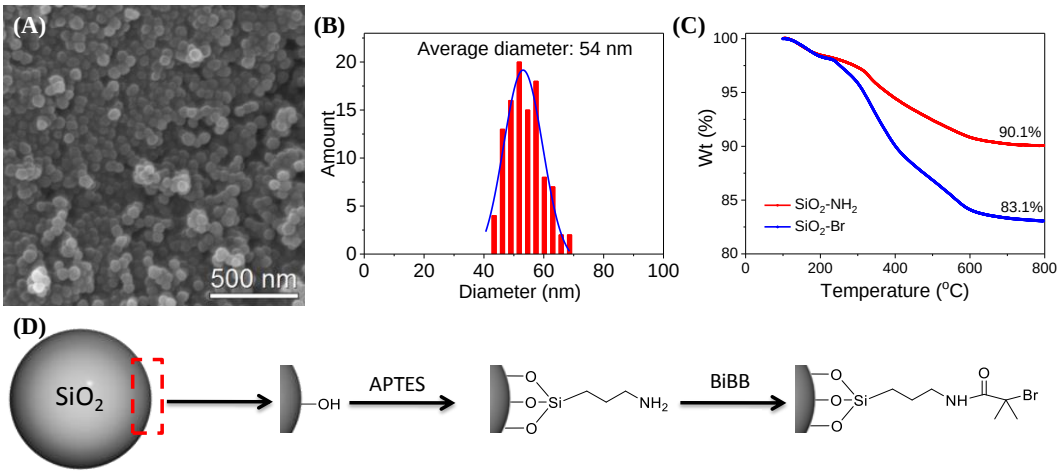

Fig. S1 (A) SEM image, and (B) particle size distribution from SEM image analysis for SiO_2 nanospheres of diameter 54 nm; (C) TGA curves for APTES-modified SiO_2 (SiO_2-NH_2) and SiO_2-Br nanospheres; (D) scheme illustration of surface modification of SiO_2 nanospheres for introducing the Br-containing ATRP initiating sites.

According to the TGA results of SiO_2-Br and SiO_2-NH_2 nanospheres in Fig. S1C, the density of Br atom on the surface of SiO_2-Br nanoparticles was calculated as follows:

$$[\mathrm{Br}] = [\mathrm{C_4H_5OBr}] = \frac{wt\%(\mathrm{C_4H_5OBr})}{\mathrm{M}(\mathrm{C_4H_5OBr})} = \frac{1 - wt\%(\mathrm{SiO_2\text{-}NH_2})}{\mathrm{M}(\mathrm{C_4H_5OBr})} = \frac{1 - \frac{83.1\%}{90.1\%}}{149}$$

$$= 0.000521\ mol\ g^{-1} = 0.521\ mmol\ g^{-1}$$

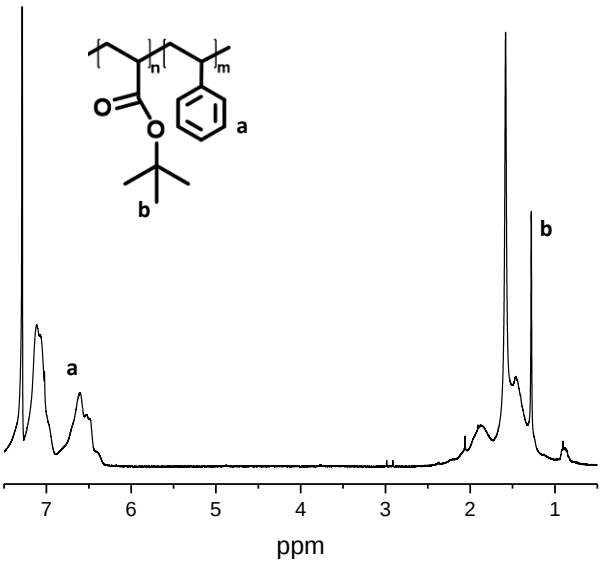

Fig. S2 ^{1}H NMR spectrum of the cleaved P*t*BA$_{81}$-*b*-PS$_{1218}$ (solvent: $CDCl_3$).

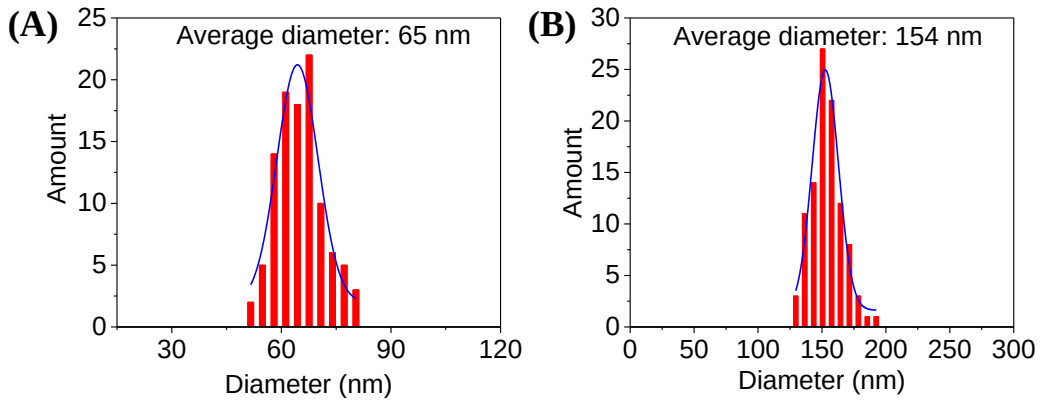

Fig. S3 Particle size distributions from SEM image analysis for (A) SiO_2-*g*-P*t*BA_{81} and (B) SiO_2-*g*-P*t*BA_{81}-*b*-PS_{1218}.

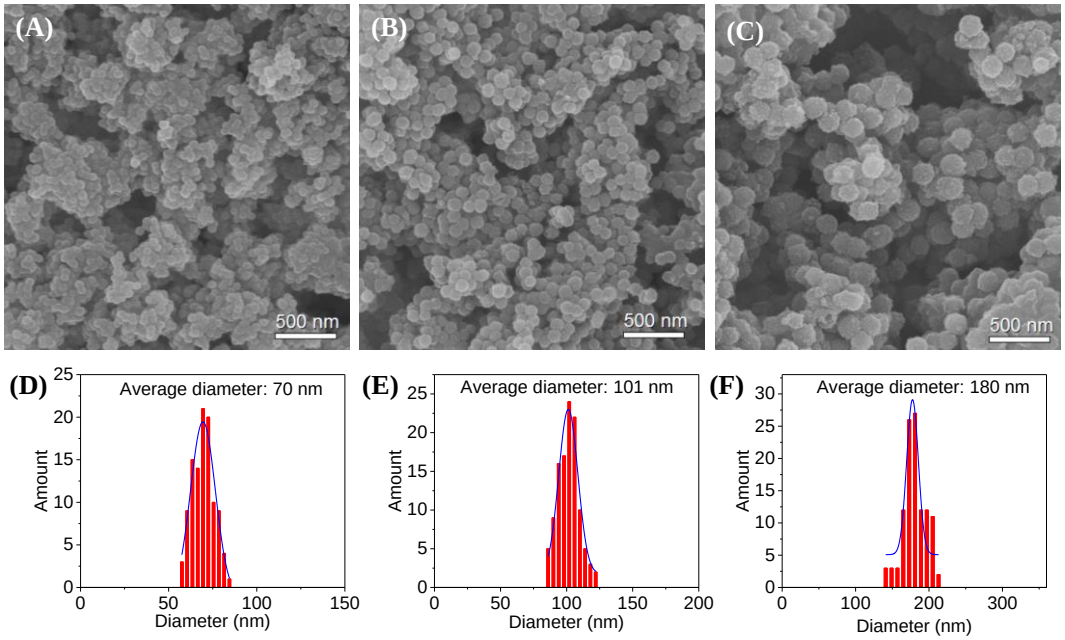

Fig. S4 SEM images and particle size distributions from SEM image analysis for (A, D) SiO_2-*g*-PAA_{81}-*b*-*x*PS_6, (B, E) SiO_2-*g*-PAA_{81}-*b*-*x*PS_{145} and (C, F) SiO_2-*g*-PAA_{81}-*b*-*x*PS_{1218}.

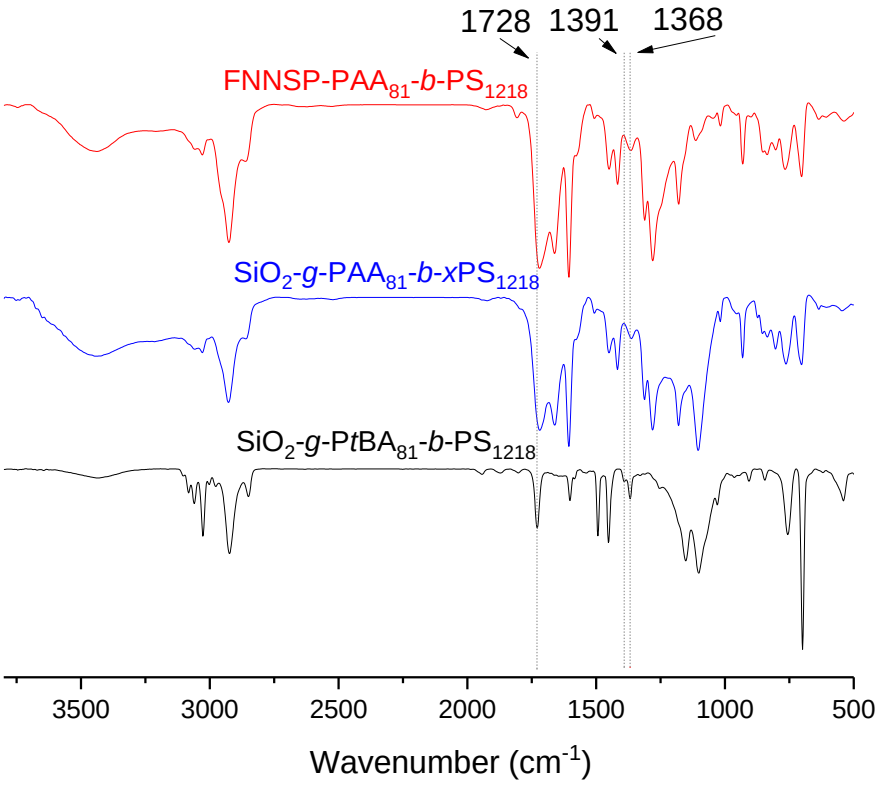

Fig. S5 Fourier transform infrared spectra for SiO_2-*g*-P*t*BA_{81}-*b*-PS_{1218}, SiO_2-*g*-PAA_{81}-*b*-*x*PS_{1218} and FNNSP-PAA_{81}-*b*-PS_{1218}.

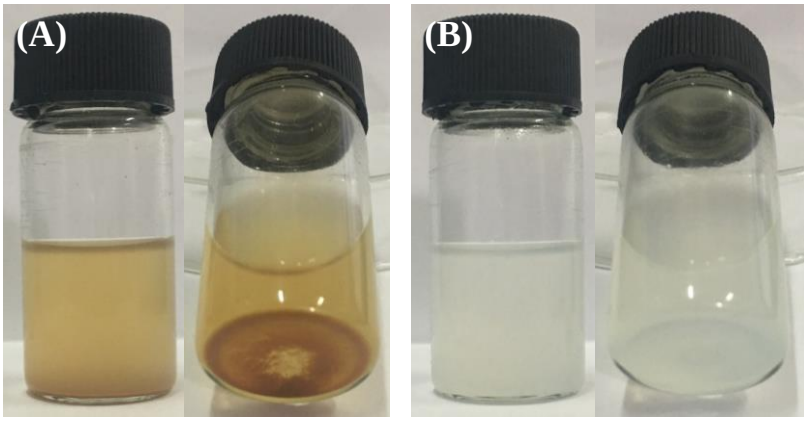

Fig. S6 Photographs of dispersions of (A) FNNSP-PAA_{81}-*b*-PS_{1218} and (B) SiO_2-*g*-P*t*BA_{81}-*b*-PS_{1218} in THF. The concentration for these two samples is 5 mg mL^{-1}.

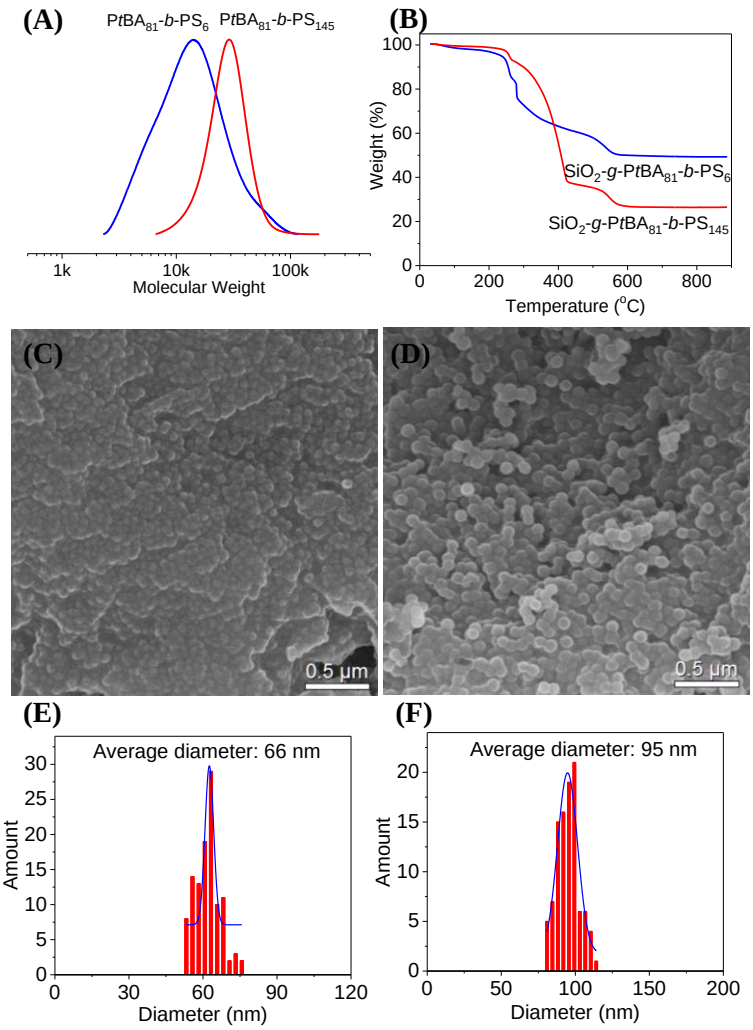

Fig. S7 (A) GPC traces of cleaved polymers and (B) TGA curves for SiO_2-*g*-P*t*BA_{81}-*b*-PS_6 and SiO_2-*g*-P*t*BA_{81}-*b*-PS_{145}; SEM images and particle size distributions from SEM image analysis for (C, E) SiO_2-*g*-P*t*BA_{81}-*b*-PS_6 and (D, F) SiO_2-*g*-P*t*BA_{81}-*b*-PS_{145}.

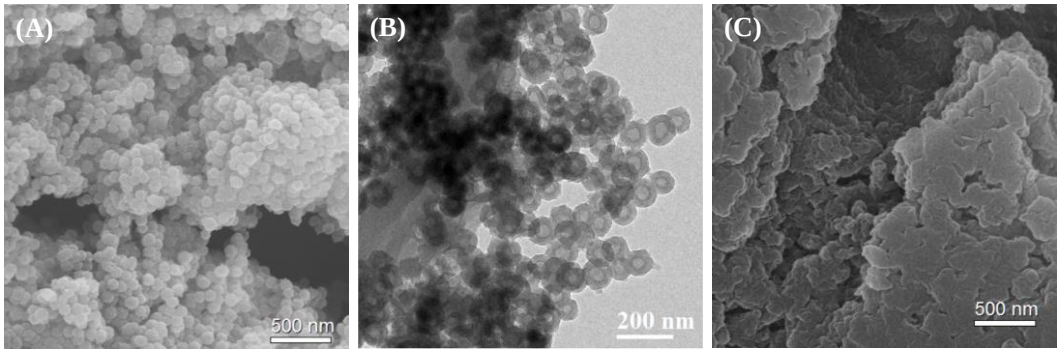

Fig. S8 (A) SEM and (B) TEM images of FNNSP-PAA_{81}-*b*-PS_{145}; (C) SEM image of FNNSP-PAA_{81}-*b*-PS_6.

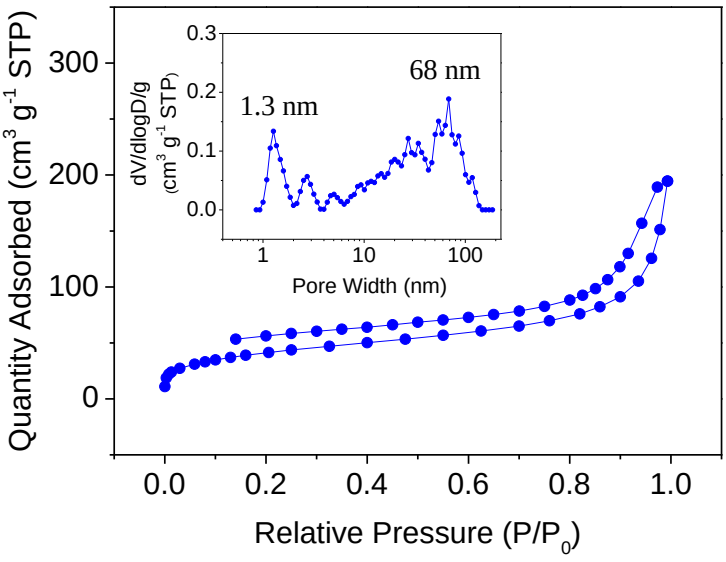

Fig. S9 N_2 adsorption-desorption isotherm and DFT pore size distribution curve (the inset) for FNNSP-PAA_{81}-*b*-PS_{145}.

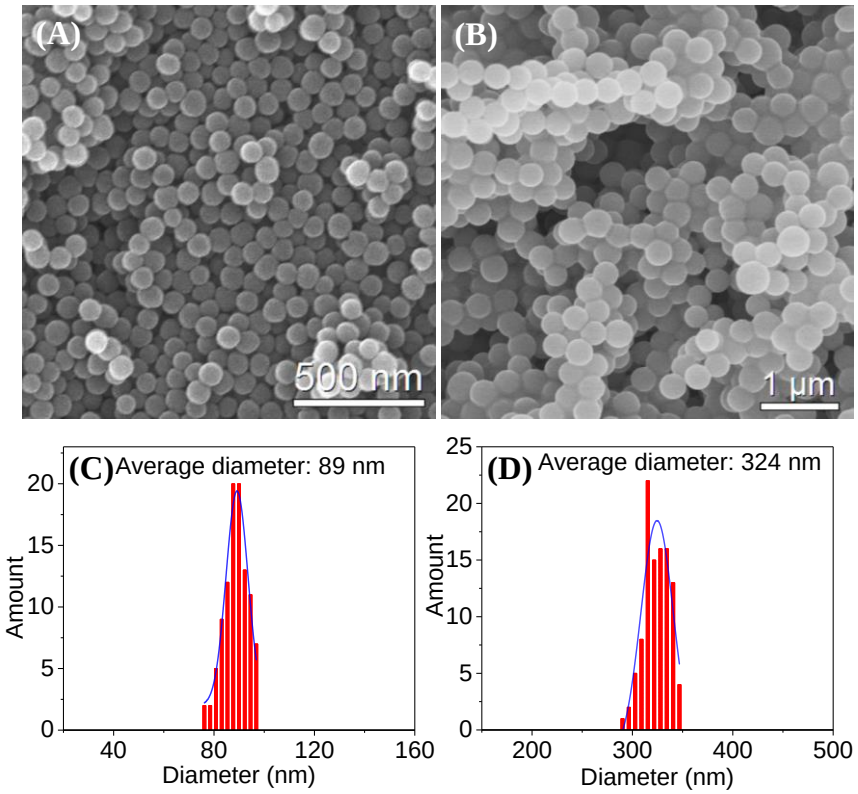

Fig. S10 SEM images and particle size distributions from SEM image analysis for SiO_2 nanosphere with diameter of (A, C) 89 nm and (B, D) 324 nm.

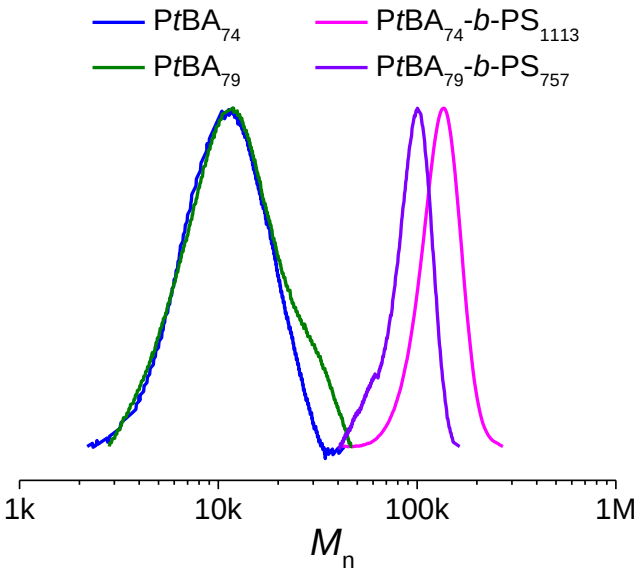

Fig. S11 GPC traces of cleaved polymers for $SiO_{2,89nm}$-*g*-P*t*BA_{74}, $SiO_{2,324nm}$-*g*-P*t*BA_{79}, $SiO_{2,89nm}$-*g*-P*t*BA_{74}-*b*-PS_{1113} and $SiO_{2,324nm}$-*g*-P*t*BA_{79}-*b*-PS_{757}.

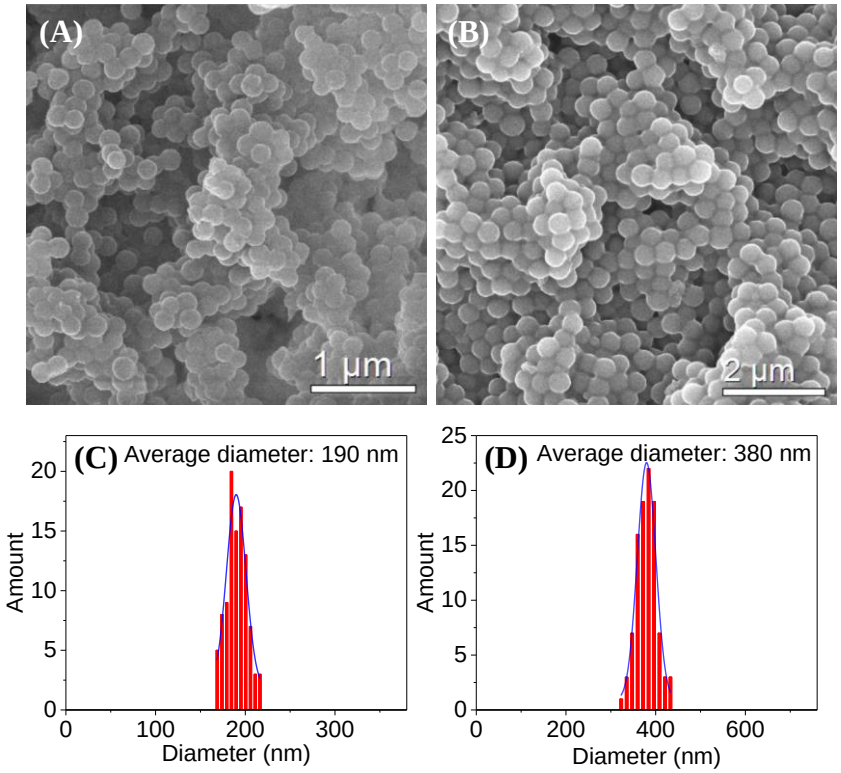

Fig. S12 SEM images and particle size distributions from SEM image analysis for (A, C) SiO_2-*g*-P*t*BA_{74}-*b*-PS_{1113} and (B, D) SiO_2-*g*-P*t*BA_{79}-*b*-PS_{757}.

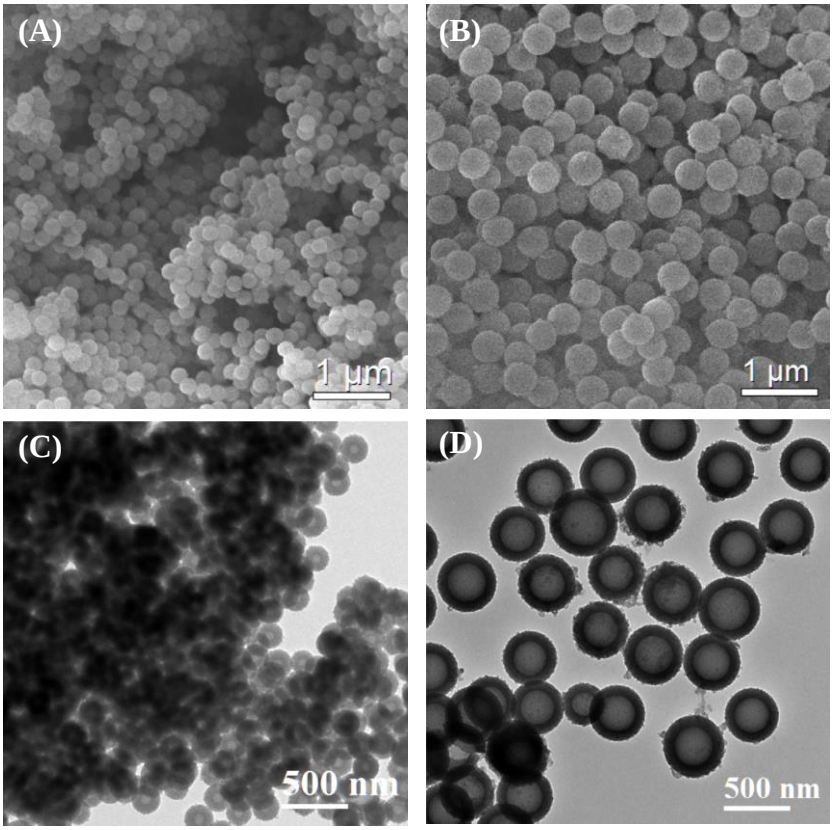

Fig. S13 SEM and TEM images of (A, C) FNNSP-P*t*BA$_{74}$-*b*-PS$_{1113}$ and (B, D) hollow microporous polymer nanosphere.

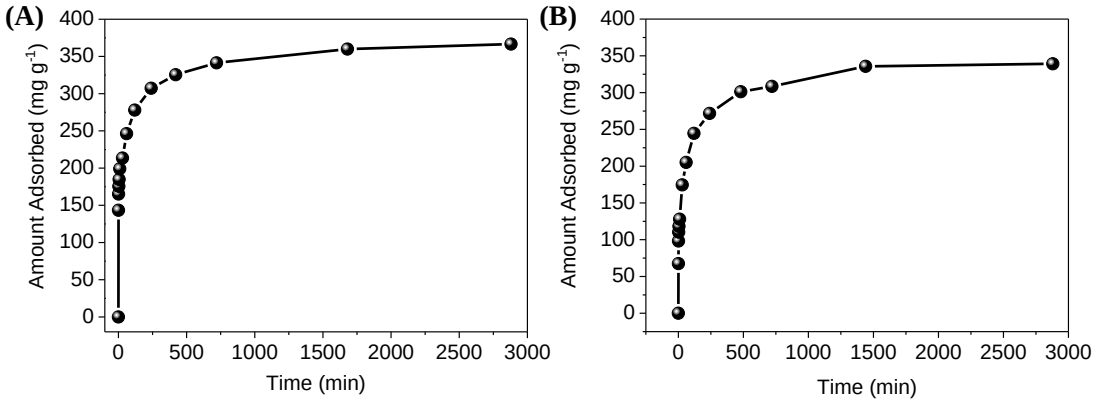

Fig. S14 Adsorption curves of FNNSP-PAA$_{81}$-*b*-PS$_{1218}$ towards (A) malachite green and (B) methyl violet solution (250 mg L^{-1}).

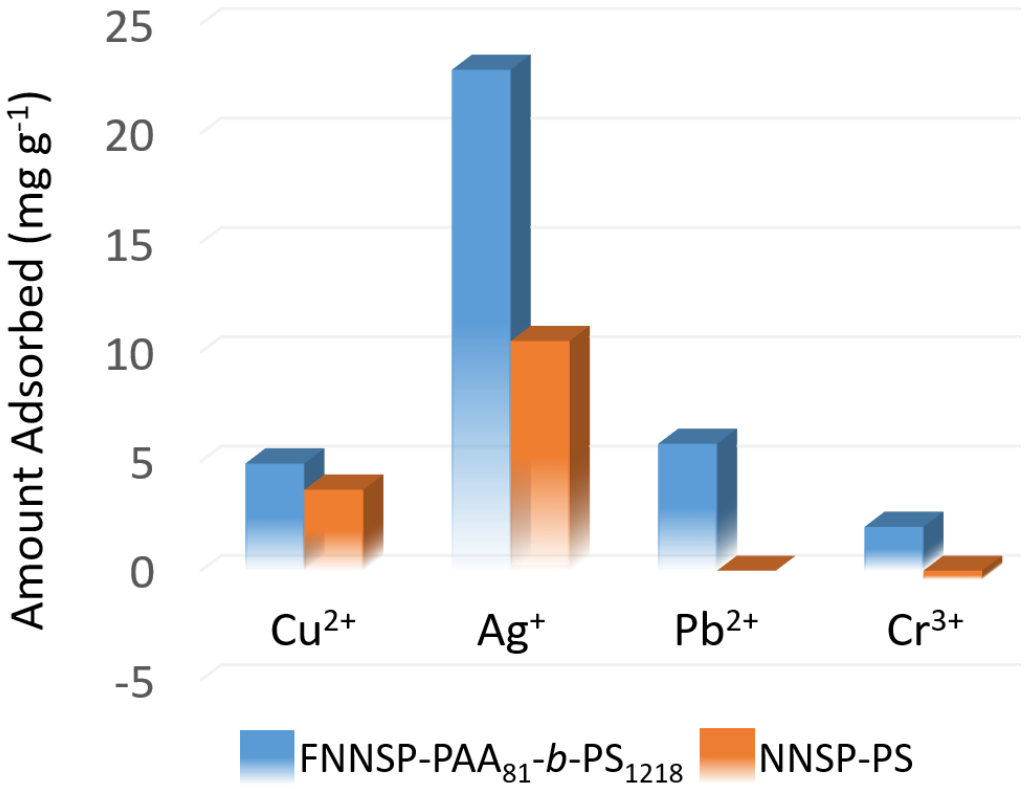

Fig. S15 Adsorption capacities of FNNSP-PAA$_{81}$-*b*-PS$_{1218}$ and NNSP-PS towards different heavy metal ions (10 ppm).

Table S1. Pore structure parameters of FNNSP-PAA products.

Sample	S_{BET} ($m^2\ g^{-1}$)	S_{mic} ($m^2\ g^{-1}$)	S_{ext} ($m^2\ g^{-1}$)	V_{total} ($cm^3\ g^{-1}$)
FNNSP-PAA_{81}-*b*-PS_{1218}	444	122	322	0.43
FNNSP-PAA_{81}-*b*-PS_{145}	150	10	141	0.30

Table S2. Summary of adsorption capacities toward malachite green (MG) and methyl violet (MV) for FNNSP-PAA_{81}-*b*-PS_{1218} and other reported adsorbents.

Adsorbent	S_{BET} ($m^2\ g^{-1}$)	$C_{0,MG}$ ($mg\ L^{-1}$)	MG adsorption capacity ($mg\ g^{-1}$)	R_{MG} (%)	$C_{0,MV}$ ($mg\ L^{-1}$)	MV adsorption capacity ($mg\ g^{-1}$)	R_{MV} (%)	Ref.
FNNSP-PAA_{81}-*b*-PS_{1218}	444	100	155	97.1	100	151	94.4	This work
FNNSP-PAA_{81}-*b*-PS_{1218}	444	250	367	91.7	250	339	84.8	This work
Activated carbon	1000	100	49.75	99.5	/	/	/	[2]
Carbon nanotube/ polyaniline composites	/	16	13.95	88	/	/	/	[3]
Graphene oxide/ cellulose bead composites	/	10	30.09	96	/	/	/	[4]
Carboxymethyl cellulose-acrylic acid	594.45	30	149.9	99.9	/	/	/	[5]
BiOI/Ag_3VO_4	36.5	25	24.25	97	/	/	/	[6]
Palygorskite modified with ammonium sulfide	190	/	/	/	300	218.11	72.7	[7]
Hydrolyzed polyacrylamide grafted xanthan gum and incorporated nanosilica	398	/	/	/	350	378.8	99.1	[8]
Activated carbon derived from phragmites australis	1362	/	/	/	75	147.02	78.4	[9]
Crosslinked starch microsphere	0.6	/	/	/	250	91.16	36.5	[10]
Granulated mesoporous carbon	960	/	/	/	20	94	94	[11]

Note: $C_{0,MG}$, R_{MG}, $C_{0,MV}$ and R_{MV} denote initial concentration of MG, MG removal efficiency, initial concentration of MV and MV removal efficiency, respectively.

Table S3. Adsorption capacities of FNNSP-PAA$_{81}$-*b*-PS$_{1218}$ and NNSP-PS towards different heavy metal ions

Sample	Cu^{2+} (mg g^{-1})	Ag^{+} (mg g^{-1})	Pb^{2+} (mg g^{-1})	Cr^{3+} (mg g^{-1})
FNNSP-PAA$_{81}$-*b*-PS$_{1218}$	4.9	22.9	5.8	2.0
NNSP-PS	3.7	10.5	0	-0.4

References

1. J. Pyun, S. Jia, T. Kowalewski, G. D. Patterson and K. Matyjazewski, *Macromolecules*, 2003, 36, 5094-5105
2. Y. Onal, C. Akmil-Basar and C. Sarıcı-Ozdemir, *J. Hazard. Mater.*, 2007, 146, 194-203
3. Y. Zeng, L. Zhao, W. Wu, G. Lu, F. Xu, Y. Tong, W. Liu and J. Du, *J. Appl. Polym. Sci.*, 2013, 127, 2475-2482
4. X. Zhang, H. Yu, H. Yang, Y. Wan, H. Hu, Z. Zhai and J. Qin, *J. Colloid Interf. Sci.*, 2015, 437, 277
5. G. Zhang, L. Yi, H. Deng and P. Sun, *J. Environ. Sci.*, 2014, 26, 1203-1211
6. S. Wang, Y. Guan, L. Wang, W. Zhao, H. He, J. Xiao, S. Yang and C. Sun, *Appl. Catal. B-Environ.*, 2015, 168, 448-457
7. G. Tian, W. Wang, Y. Kang and A. Wang, *J. Environ. Sci.*, 2016, 41, 33-43
8. S. Ghorai, A. Sarkar, M. Raoufi, A. B. Panda, H. Schonherr and S. Pal, *ACS Appl. Mater. Interfaces*, 2014, 6, 4766-4777
9. S. Chen, J. Zhang, C. Zhang, Q. Yue, Y. Li and C. Li, *Desalination*, 2010, 252, 149-156
10. Q. Lin, J. Pan, Q. Lin and Q. Liu, *J. Hazard. Mater.*, 2013, 263, 517-524
11. Y. Kim, J. Bae, H. Park, J. Suh and Y. You, *Water Res.*, 2016, 101, 187-194